Journal of
Materials Chemistry A

Accepted Manuscript

This article can be cited before page numbers have been issued, to do this please use: E. Sánchez-González, P. Mileo, M. Sagastuy-Breña, J. R. Álvarez, J. Reynolds III, A. Villarreal, A. Gutierrez-Alejandre, J. Ramirez, J. Balmaseda, E. González-Zamora, G. Maurin, S. M. Humphrey and I. A. Ibarra, *J. Mater. Chem. A*, 2018, DOI: 10.1039/C8TA05400B.

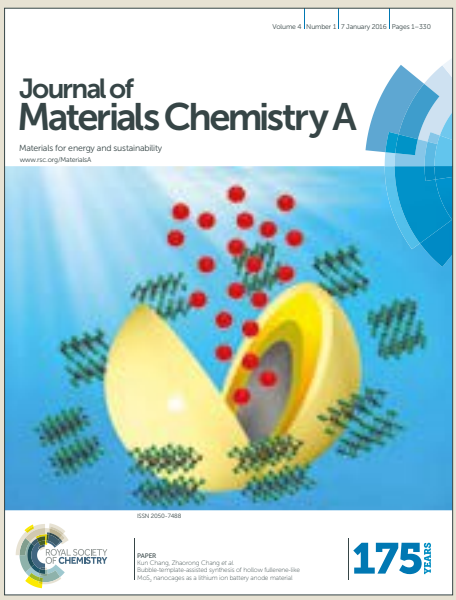

ROYAL SOCIETY OF CHEMISTRY

rsc.li/materials-a

View Article Online
DOI: 10.1039/C8TA05400B

TOC

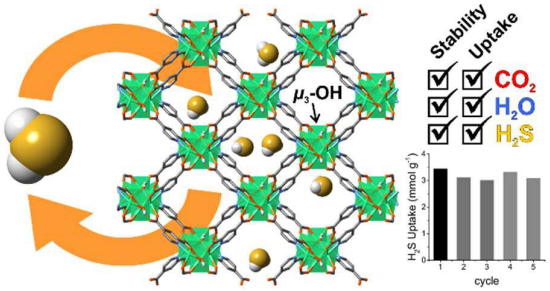

Mg-CUK-1 exhibited high chemical stability towards H_2S and H_2O. The highly reversible H_2S uptake, at 303 K, was highly correlated with Monte Carlo Simulations.

View Article Online
DOI: 10.1039/C8TA05400B

Journal of Materials Chemistry A

ARTICLE

Highly reversible sorption of H_2S and CO_2 by an environmentally-friendly Mg-based MOF

Received 00th January 20xx,
Accepted 00th January 20xx

DOI: 10.1039/x0xx00000x

www.rsc.org/

Elí Sánchez-González,[a,‡] Paulo G. M. Mileo,[b,‡] Mónica Sagastuy-Breña,[a] J. Raziel Álvarez,[a] Joseph E. Reynolds III,[c] Aline Villarreal,[d] Aída Gutiérrez-Alejandre,[d] Jorge Ramírez,[d] Jorge Balmaseda,[a] Eduardo González-Zamora,[e] Guillaume Maurin,[b,*] Simon M. Humphrey[c,*] and Ilich A. Ibarra[a,*]

Mg-CUK-1, an ecologically-friendly material synthesized in water is found to be a high-capacity, highly reversible adsorbent for acidic gases including H_2S and CO_2. Furthermore, Mg-CUK-1 is demonstrated to retain long-range crystallinity upon sorption cycling; its sorption performance is retained over multiple cycles, even in the presence of high relative humidity (95%). Reversible H_2S adsorption by Mg-CUK-1 is rare among MOFs studied for this purpose to-date. The joint experimental and computational stuies presented here show that Mg-CUK-1 is an effective solid adsorbent for applications in the field of acid gases capture, an application that is highly relevant for the purification of many industrial gas streams.

Introduction

The development of new functional materials for environmental remediation applications such as the capture of toxic gaseous by-products is an important issue for many large-scale industrial processes.[1] There is a continuing need to improve the performance of such materials, as well as to determine ways to manufacture them using environmentally-sensitive and realistically scalable methods. Metal-Organic Frameworks (MOFs) are a topical class of crystalline solids[2a] that can be synthesised with 3-D microporous structures, making them ideal candidates for toxic gas remediation applications.[2c,b] MOFs have already shown promise in the selective capture of a variety of pollutants of direct relevance to air quality, climate change, and human health in modern society.[3] By tailoring the chemical functionality of the MOF pore environment, the sorption behaviour of a given MOF can be fine-tuned for highly selective storage and/or separation of specific gaseous pollutants, including CO_2,[4] H_2S,[5] SO_2,[6] NH_3,[7] NO_x,[8] and volatile organic compounds (VOCs).[3,5a,9,10] Despite their potential utility, the vast majority of MOFs must be synthesised using harmful organic solvents (*e.g.*, *N,N´*-dimethylformamide, DMF),[11] in direct conflict with the primary motivations of using such materials to address environmental issues. Thus, the preparation of functional MOFs using green synthetic strategies, *i.e.*, using water as a solvent and non-toxic metal and organic components, is of timely importance.[12]

[a] *Laboratorio de Fisicoquímica y Reactividad de Superficies (LaFReS), Instituto de Investigaciones en Materiales, Universidad Nacional Autónoma de México, Circuito Exterior s/n, CU, Del. Coyoacán, 04510, Ciudad de México, Mexico. E-mail: argel@unam.mx; Fax: +52(55) 5622-4595.*
[b] *Institut Charles Gerhardt Montpellier, UMR-5253, Université de Montpellier, CNRS, ENSCM, Place E. Bataillon, 34095 Montpellier cedex 05, France. E-mail: guillaume.maurin@univ-montp2.fr*
[c] *Department of Chemistry, The University of Texas at Austin, Welch Hall 2.204, 105 East 24th St., Stop A5300, Austin, Texas 78712-1224, United States. E-mail: smh@cm.utexas.edu*
[d] *UNICAT, Departamento de Ingeniería Química, Facultad de Química, Universidad Nacional Autónoma de México (UNAM), Coyoacán, Ciudad de México, Mexico.*
[e] *Departamento de Química, Universidad Autónoma Metropolitana-Iztapalapa, San Rafael Atlixco 186, Col. Vicentina, Iztapalapa, C. P. 09340, Ciudad de México, Mexico.*

† Electronic Supplementary Information (ESI) available: TGA data, PXRD data, SEM micrographs, breakthrough plots, DRIFT-FTIR spectra and molecular simulations. See DOI: 10.1039/x0xx00000x

‡ These authors contributed equally to this work.

View Article Online
DOI: 10.1039/C8TA05400B

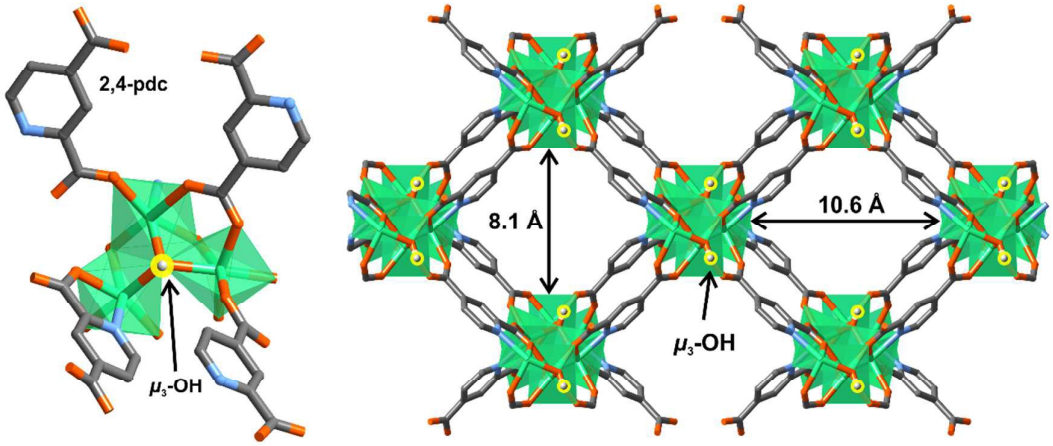

Figure 1. (left) view of the trinuclear building block of three Mg(II) metal ions oxygen-octahedra bridged by a μ_3-hydroxyl group, through the *b* axis, and (right) the crystal structure of Mg-CUK-1 along *c* axis showing 8.1 x 10.6 Å channels.

Hydrogen sulfide (H_2S) is a toxic species present in natural gas and biogas; the desulfurization process of different gas streams, (*e.g.*, oil refineries) is a primary source of H_2S emissions.[5b] H_2S is a colourless gas, which is highly corrosive, flammable and poisonous to humans. At concentrations over 100 ppm, H_2S can be lethal since this molecule is quickly absorbed into the blood stream, limiting O_2 uptake at the cellular level.[13] Therefore, the selective capture of H_2S is essential in many industrial processes. However, only very few porous materials have been comprehensively studied in H_2S capture to-date.[5a,b] Representative studies reported by De Weireld,[14] Zou[15] and Eddaoudi[16] indicate that most of the MOFs undergo decomposition upon adsorption of H_2S, while it is difficult for some others to desorb H_2S due to relatively strong host-guest binding in the pores either *via* strong physisorption or even by chemisorption. In this case, desorption of H_2S is therefore accompanied by an impractically large energy penalty.[17] The identification of new MOFs that are capable of highly cyclable H_2S sequestration under industrially-feasible pressure-swing desorption conditions[18a] remains an important, unsolved problem. CO_2 is another topical acidic gas that is commonly present alongside H_2S in industrial gas streams (*e.g.*, in natural gas and syngas).[18b] Thus, there is a critical need to design new adsorbents that can reversibly capture both H_2S and CO_2 with high capacities, under industrially-realistic conditions.

Perhaps the most vitally important consideration regarding the potential use of MOFs as H_2S and CO_2 adsorbents under industrially-realistic relates to their stability in the presence of ambient moisture. Effluent gas streams that require scrubbing for H_2S and other toxic molecules commonly contain high relative humidity (%RH). This presents a major problem to MOFs that are susceptible to hydrolysis.[19a] As a potential solution to this problem, it has been shown that MOFs constructed using highly polarizing and high-valent metal cations (*e.g.*, Mg^{2+}, Cr^{3+}, Al^{3+}, Ti^{4+}, Zr^{4+}) exhibit enhanced chemical stability in the presence of moisture.[19b,c] Other examples of water-stable MOFs include those recently reported by Dincă *et al.*[19d], Eddaoudi *et al.*[19e] and Uribe-Romo *et al.*[19f] who showed outstanding water adsorption performances. Such hydrolytic stable MOFs could also be employed in a number of other critical large-scale applications, as adsorbents in heat-pumps and chillers,[20] in storage technologies for arid environments,[21] in low-cost water capture and abatement,[22] and in water-mediated proton conductors.[23]

In this contribution, we show that an environmentally-friendly Mg(II)-based MOF can reversibly adsorb H_2S and CO_2 gases with high storage capacities, between 0–1 bar. The MOF, called Mg-CUK-1[24] (CUK = Cambridge University–KRICT), originally reported by Humphrey and co-workers, can be prepared rapidly (30 min) in large quantities under microwave-assisted heating, using only water as the solvent.[24] Mg-CUK-1 is also of relatively low toxicity, since it is only comprised of Mg(II) ions coordinated to the commercially-available organic ligand 2,4-pyridine dicarboxylic acid (2,4-pdcH_2; C_5H_3N-2,4-CO_2H) and hydroxide ions (OH^-). Mg-CUK-1 was shown to be unusually thermally stable (>500 °C) owing to the presence of infinite chains of edge- and vertex-sharing $[Mg_3(\mu_3\text{-}OH)]^{5+}$ triangles that support corrugated 1-D channels with a cross-sectional accessible opening of 8.1 x 10.6 Å (Figure 1).[24] Based on the solvent of synthesis, Mg-CUK-1 is inherently water-stable and it can be rehydrated by direct immersion in aqueous media.

In this work, to test the viability of Mg-CUK-1 in the reversible capture of the acidic gases CO_2 and H_2S as well as the adsorption of CO_2 in the presence of relative humidity, we carefully characterised the following features: (*i*) the H_2O adsorption-desorption properties to evaluate the impact of humidity on the material; (*ii*) the CO_2 capture properties under controlled RH; and, (*iii*) the H_2S sequestration performance upon multiple cycles of adsorption and desorption. To support these application-focused experimental studies, we have employed advanced computational methods to gain fundamental insights into the mechanisms responsible for the

View Article Online
DOI: 10.1039/C8TA05400B

observed reversible sorption of H_2S and CO_2 by Mg-CUK-1 under operating conditions.

EXPERIMENTAL SECTION

Chemicals

2,4-Pyridinedicarboxlic acid (2,4-pdcH_2), magnesium nitrate hydrate ($Mg(NO_3)_2$) and potassium hydroxide (KOH) were purchased from Sigma-Aldrich and used as received. *In-house* deionized water was used to prepare all solutions. For sorption studies, ultra-high purity (99.9995+%) N_2 and CO_2 gases as well as H_2S (15.0 % vol. diluted in N_2) were obtained from Praxair.

Material Synthesis

Mg-CUK-1, $[Mg_3(\mu_3\text{-}OH)_2(2,4\text{-}pdc)_2]$, was synthesised following the previously reported procedure.[24] In brief, 2,4-pdc (170 mg; 1.0 mmol) was dissolved in H_2O (4.0 cm^3) by the addition of KOH (2.0 M; 2.0 cm^3), to which was added a second solution of $Mg(NO_3)_2$ hydrate (380 mg; 1.5 mmol) in H_2O (4 cm^3) to give a viscous, opaque white slurry. The mixture was transferred into a Teflon-lined Easy-Prep (CEM Corp.) vessel and heated at 573 K for 35 min in a MARS microwave reactor (CEM Corp.). The reaction temperature was controlled using a fiber-optic sensor. After cooling to room temperature (15–30 min), the crystalline solid was purified by short (3 x 20 s) cycles of sonication in fresh H_2O, followed by decanting away the amorphous suspension. Large, colourless prismatic crystals were isolated (average yield = 124 mg, 42%). Thermogravimetric analysis (TGA) and powder X-ray diffraction (PXRD) of the sample were carried out to confirm phase purity of the Mg-CUK-1 (Figs. S1 & S2).

Adsorption Isotherms for CO_2 and H_2O

CO_2 sorption isotherms (196 K and up to 1 bar) were performed on a Belsorp HP analyser under high vacuum in a clean system. The estimated BET area ($0.005 < P/P_0 < 0.15$) was equal to 604 $m^2\ g^{-1}$ with a corresponding pore volume of 0.22 $cm^3\ g^{-1}$ (Fig. S3). These textural properties are in good agreement with the previously reported data.[24,25] This correlation confirmed the correct activation of the material. High pressure CO_2 adsorption isotherms (0–6 bar, and 303 K) were collected on a Belsorp HP analyser. H_2O vapour isotherms were recorded by a dynamic method, using air gas as carrier gas, in a DVS Advantage 1 instrument from Surface Measurement System (mass sensitivity: 0.1 µg, Relative Humidity (RH), accuracy: 0.5 %RH, vapour pressure accuracy: 0.7 %P/P_0. Mg-CUK-1 samples were activated at 373 K for 1 hour under flowing N_2. The H_2O uptake in weight percent (wt%) units was calculated as [(adsorbed amount of water) / (amount of adsorbent) X 100], consistent with established procedures. Water cycling experiments were performed at 303 K; for the adsorption phase, RH = 95% was maintained for 8 hours. Then, the sample was exposed to a dry air flow for a further 8 hours to ensure complete desorption prior to re-adsorption. CO_2 adsorption experiments at fixed RH were performed on the hydrated Mg-CUK-1 (13% RH). The material was activated as described above and then exposed to this constant RH for 1 hour. The water-impregnated sample was then transferred to a Belsorp HP analyser cell to undertake the CO_2 adsorption.

H_2S Adsorption-Desorption Studies

Dynamic adsorption experiments were performed at 303 K using a tubular quartz adsorber (internal diameter = 7 mm) filled with Mg-CUK-1 (Scheme S1). Before beginning the H_2S adsorption tests, samples were activated *in situ* at 373 K for 1 hour with a constant flow of dry N_2 gas and then slowly cooled to 303 K. Samples were exposed to synthetic H_2S/N_2 gas mixtures at p = 0.689 bar with a total flow rate = 30 $cm^3\ min^{-1}$. A HP-5890 gas chromatograph equipped with an HP-PLOT 1 column and TCD was used to analyse the H_2S concentration. Adsorption experiments at different H_2S concentrations were performed using 6, 9, 12 and 15 %vol. H_2S/N_2 gas mixtures (see ESI for the corresponding breakthrough curves). The adsorption capacities were obtained by integrating the areas above the breakthrough curves. At the end of each experiment, the Mg-CUK-1 sample was exposed to a constant flow of dry N_2 gas, after which the sample was put through a Temperature Swing Re-activation (TSR) cycle (under N_2 gas) at 373 K using the standard protocol (*vide supra*) prior to changing the H_2S vol%.

DRIFTS

Diffuse-reflectance infrared Fourier-transform spectroscopy (DRIFTS) of Mg-CUK-1 samples in powder form were measured using a Nicolet 380 spectrometer (DTGS detector) with 4 cm^{-1} resolution equipped with a diffuse reflectance vacuum cell fitted with KBr windows. DRIFT spectra were collected on an activated Mg-CUK-1 sample (373 K for 1 h and ~6 x 10^{-3} Torr), as well as of the same sample after exposure to five cycles of H_2S adsorption-desorption. To do so, as-synthesised Mg-CUK-1 was first activated and exposed to H_2S using the protocol described above; after the fifth reactivation, the powder was transferred to a quartz cell and briefly evacuated at 6 x 10^{-3} Torr at 303 K before collecting the spectrum.

Scanning Electron Microscopy (SEM)

Morphology studies were carried out in a JEOL Benchtop Scanning Electron Microscope, Neoscope JCM-6000 using secondary electrons at 15 kV current, in high vacuum, and the process of the images was carried out by the Neoscope software.

View Article Online
DOI: 10.1039/C8TA05400B

Computational Details

The crystal structure of Mg-CUK-1[24] (CCDC-1024710) was geometry-optimized at the density functional theory (DFT) level while keeping the experimental cell parameter fixed. These calculations employed a PBE functional[26] combined with a double numeric basis set containing polarization functions (DNP),[27a] as implemented in the Dmol^3 package. The same settings were employed to geometry-optimize the H_2S-loaded Mg-CUK-1 at different guest concentrations. The partial charges (Fig. S6) for each atom in the MOF were derived from the REPEAT strategy (see ESI).[27b]

The microscopic models of the three guest molecules were defined as follows: (*i*) CO_2 was described by the EPM2 model,[28] corresponding to a rigid and linear molecule representation with 3 charged Lennard-Jones (LJ) sites and a C=O bond length of 1.149 Å; (*ii*) H_2O was represented by the TIP4P/2005 model,[29] a four-site model, with a single LJ site centered in the oxygen position and three charged sites, two centered in the hydrogen positions and one located 0.1546 Å below the hydroxyl-O atom in the molecule bisector axis, having an O–H bond length of 0.9572 Å; and, (*iii*) H_2S was represented by the model reported by Kammath *et al.* (2005),[30] *i.e.*, using a model with three charged LJ sites centered in the atomic position, a S–H bond of 1.34 Å, and an H–S–H bond angle = 92.5°. Regarding CUK-1, the 12-6 LJ parameters for the inorganic and organic moieties were taken from the UFF[31] and DREIDING[32] force fields, respectively. The Mg-CUK-1/guest interactions were described using a 6-12 LJ potential, and a coulombic contribution. Following a general approach adopted in previous studies,[33] the H atom of the μ_3-OH groups interacts with the guests only through electrostatic interactions. The LJ crossed parameters between the MOF and the guests were calculated using the Lorentz-Berthelot mixing rules. The LJ contribution had a cut-off distance of 12 Å, while long-range electrostatic interactions were handled using the Ewald summation technique.[34]

Next, Grand Canonical Monte Carlo (GCMC) simulations were carried out at 303 K to predict the adsorption behaviour of Mg-CUK-1 for H_2O, CO_2 and H_2S as single components. A simulation box made of 12 unit cells (3 x 2 x 2) was employed, by fixing all atoms of the framework in their initial positions. The adsorption enthalpies at low coverage were calculated using the revised Widom's test particle insertion method.[35] As a further step, in order to gain insight on the CO_2 adsorption properties of CUK-1(Mg) in the presence of H_2O, GCMC simulations were performed for a MOF framework loaded with 1 H_2O molecule *per* unit cell (corresponding to the experimental water loading at 13% RH). In the case of H_2S, additional MC simulations were performed in the canonical ensemble (NVT) to identify the preferential adsorption sites for the guest molecules at low, intermediate and high pressures. This exploration involved the analysis of the radial distribution functions plotted between different MOF/guest pairs calculated from hundreds of MC configurations.

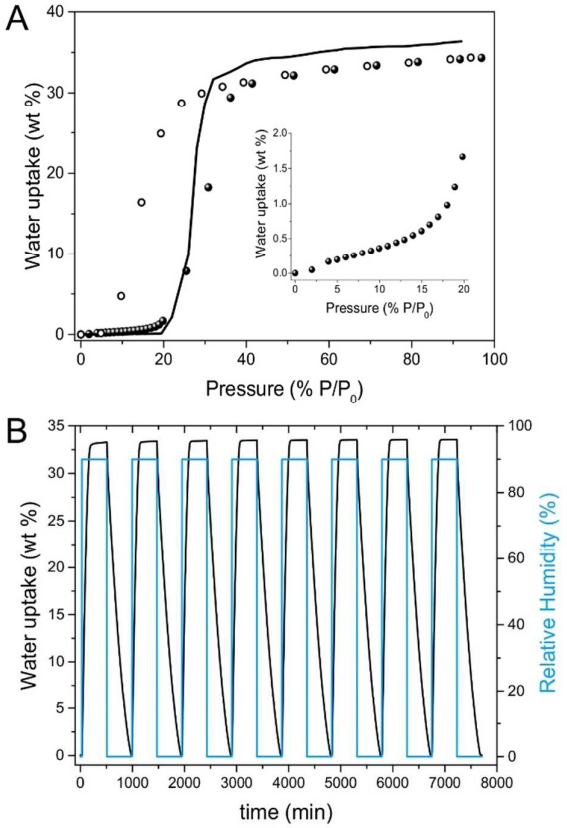

Figure 2. A Water adsorption isotherm at 303 K of Mg-CUK-1 from %P/P_0 = 0 to 95. Solid and open circles represent experimental adsorption and desorption branches respectively and the solid line represents the GCMC simulations of the adsorption. The inset shows the H_2O adsorption isotherm at 303 K from %P/P_0 = 0 to 20. **B** Water adsorption-desorption uptake obtained from 8 cycles on Mg-CUK-1 at 303K.

Results and Discussion

Figure 2A shows the water adsorption isotherm of Mg-CUK-1 between 0–95% P/P_0, obtained at 303 K. The isotherm corresponds to a Type-V adsorption behaviour: at low pressure (0–20% P/P_0) H_2O adsorption is very gradual (Figure 2A, inset); then, there is a rapid increase in H_2O uptake between 20–35 %P/P_0; above 35% P/P_0 the uptake remained basically constant corresponding to a maximum H_2O uptake of 34.4 wt% (19.1 mmol g^{-1} at 95% P/P_0). This performance is among the best MOFs reported so far (adsorption uptake ranging from 25 to 40 wt%)[21,36,37] for low-cost atmospheric water generation, although the material Co_2Cl_2BTDD has achieved 96 wt%.[38]

View Article Online
DOI: 10.1039/C8TA05400B

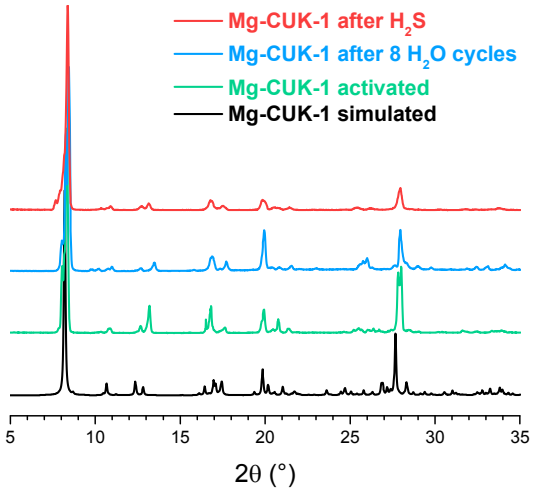

Figure 3. PXRD patterns of the Mg-CUK-1 simulated pattern from the crystal structure (black line), activated sample (green line), after H_2O sorption cycling (blue line), and after H_2S sorption (red line).

These experimental data obtained for Mg-CUK-1 are in excellent agreement with the GCMC-predicted adsorption isotherm (Figure 2A; solid line), which provides a solid validation of the microscopic model (LJ parameters and charges) employed in our simulations for the CUK-1 framework. Such a shape of the adsorption isotherm is due to a mildly hydrophilic character of Mg-CUK-1, as confirmed by a moderate simulated adsorption enthalpy for H_2O at very low coverage (–42.6 kJ mol^{-1}) which then increases up to -60 kJ mol^{-1} above P/P_0 = 0.20. Furthermore, one observes a well-pronounced hysteresis loop upon desorption (Figure 2A; open circles) mostly caused by the presence of strong H-bonding between the H_2O adsorbates and the hydroxyl groups that are present once the pore starts to be filled.[39] Since the accessible pore openings of Mg-CUK-1 (8.1 x 10.6 Å)[24] are significantly larger than the kinetic diameter of H_2O (2.7 Å), the observed hysteresis is unlikely due to `kinetic trapping´ behaviour.[40-42]

To investigate the H_2O adsorption-desorption cyclability of Mg-CUK-1, a set of eight H_2O sorption isotherms were measured continuously on the same sample at 303 K (Figure 2B). This study showed no apparent decrease in the total capacity, indicating that Mg-CUK-1 can be repeatedly fully dehydrated. The water was successfully removed between each cycle by simply flowing dry N_2 through the sample, without the need to use additional external heating. This method of regeneration is highly beneficial from an energy economy perspective. PXRD analysis of the same Mg-CUK-1 sample after eight adsorption-desorption experiments confirmed retention of bulk crystallinity (Figure 3; blue data). Additionally, a CO_2 adsorption isotherm at 196 K was collected on the sample that underwent 8 water adsorption cycles to assess the retention of its surface area under this operating condition (Fig. S4). The estimated BET area was equal to 586 m^2 g^{-1}, which is very similar to the value obtained for the pristine material (604 m^2 g^{-1}), *i.e.* only a 3% loss of surface area. This emphasizes the exceptional stability of Mg-CUK-1 in the presence of water vapour.

CO_2 Adsorption Studies

Next, isothermal adsorption CO_2 experiments were performed on Mg-CUK-1 as a function of % RH. A comparison of the CO_2 adsorption isotherms at 303 K obtained for the fully dehydrated Mg-CUK-1 versus Mg-CUK-1 rehydrated to 13% RH are presented in Figure 4. The total adsorbed amount of CO_2 was very similar in both cases between 0–0.3 bar. At higher partial pressures, there was a slight enhancement in CO_2 uptake for the sample at 13% RH, which reaches 3.37 mmol g^{-1} at 1 bar (*cf.* 3.03 mmol g^{-1} for the anhydrous sample at the same pressure; Figure 4). At elevated pressures (2–6 bar of CO_2), the uptake difference remained approximately constant, reaching a total uptake of 5.89 and 6.39 mmol g^{-1} for the anhydrous and partially hydrated samples, respectively. Both experimental adsorption isotherms were very well reproduced by our GCMC simulations, from which we were also able to extract a relatively high CO_2 adsorption enthalpy of –35 and –36.5 kJ mol^{-1} for the anhydrous and partially hydrated samples, respectively; these magnitudes are in-line with what has been reported experimentally and theoretically for other μ_3-OH-decorated MOFs that show specific interactions between these hydroxyl groups and the CO_2 molecules.[43] Interestingly, these results clearly demonstrated that the CO_2 adsorption properties of Mg-CUK-1 in terms of both CO_2 uptake and affinity are retained in the presence of humidity. This is in sharp contrast with some other CO_2 adsorbents which show a drastic drop of their performances in the presence of humidity.[44] We can assume that adsorbed water binds to the μ_3-OH groups that create additional adsorption sites for CO_2 molecules and hence contribute to slightly enhance both CO_2 adsorption capacity and affinity as previously observed.[39] This

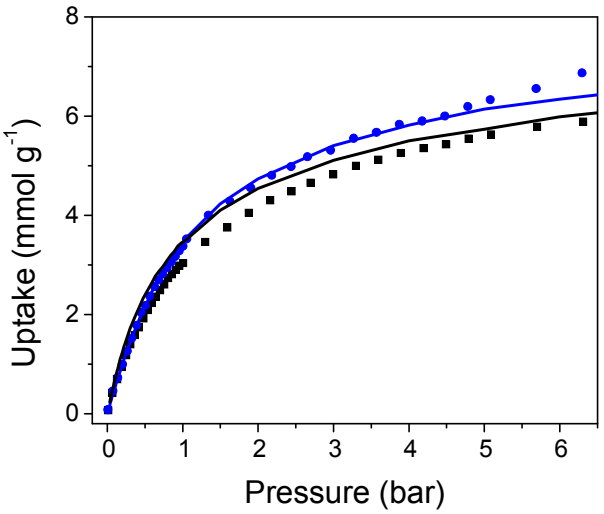

Figure 4. Experimental CO_2 adsorption isotherm for fully dehydrated Mg-CUK-1 (black squares) and Mg-CUK-1 in the presence of 13% RH (blue circles); the corresponding simulated adsorption isotherms are represented as solid lines. All data are reported at 303 K.

View Article Online
DOI: 10.1039/C8TA05400B

renders Mg-CUK-1 as an attractive adsorbent to operate the capture of CO_2 in real conditions.

H_2S Adsorption Studies

The adsorption of H_2S by Mg-CUK-1 was assessed by a series of breakthrough experiments (see ESI). The adsorption capacities obtained are shown in Fig. S8. At the lowest H_2S concentration studied (6 %vol. H_2S), the gas uptake was equal to 1.41 mmol H_2S g^{-1}, which corresponds to 45.5 cm^3 H_2S g^{-1}. This value is approximately the same as the N_2 adsorption capacity observed at the same pressure.[24] The H_2S uptake by Mg-CUK-1 was approximately 40% higher than the performances of a number of well-studied MOFs (experiments with low H_2S concentrations *ca.* 1–6 kPa), including MIL-100(Fe),[15] MIL-53(Fe),[14] HKUST-1,[15] MOF-5[15], MIL-53(Cr)[14], Ga-soc-MOF[16] and MIL-125(Ti),[45] all of which show H_2S capacities of approximately 1 mmol g^{-1}. Similar H_2S capacities have been reported for Zn-MOF-74 (1.64 mmol g^{-1})[15] and Cu(BDC)(TED)$_{0.5}$ (1.65 mmol g^{-1}).[15] Notably, of this entire list of MOFs, only MIL-53(Cr) and Ga-soc-MOF were able to reversibly adsorb H_2S in addition to Mg-CUK-1, which is an essential condition for their potential use in practical applications. In order to validate our experimental H_2S breakthrough adsorption results, we evaluated the H_2S adsorption performances of MOF-74, HKUST-1 and MIL-101(Cr), which were previously explored using H_2S breakthrough experiments. Our home-made experimental setup revealed very similar H_2S capture performances to the existing data (see Fig. S9 and Table S2), demonstrating the reliability of our measurements.

Interestingly, Mg-CUK-1 also exhibited a two-fold increase in its H_2S adsorption capacity as the H_2S feed gas concentration was increased from 6 to 15 %vol (reaching 3.1 mmol H_2S g^{-1}); 15 vol% is the maximum feed concentration that could be practically measured (equivalent to 0.1 bar of H_2S). In order to investigate the H_2S regeneration-capacity and the structure stability of Mg-CUK-1, cycling H_2S experiments at 15 %vol H_2S were then performed on the same Mg-CUK-1 sample; this was accompanied by PXRD and scanning electron microscopy (SEM) analyses of the products to confirm retention of the crystal structure (Figure 3 red data and Fig. S13). First, cycling adsorption-desorption results showed that the H_2S adsorption capacity remained constant during the five adsorption-desorption cycles (3.2±0.2 mmol g^{-1}, Figure 5A), which suggests that H_2S was completely desorbed when the sample was re-activated. A comparison of the DRIFTS data for the as-synthesised Mg-CUK-1 and H_2S-cycled Mg-CUK-1 samples after re-activation (at 373 K for 1 h under flowing N_2 gas) led to spectra that were essentially indistinguishable (Fig. S15), confirming that this re-activation condition allows the full removal of H_2S. Since the adsorption capacity did not change after several adsorption-desorption cycles, Mg-CUK-1 appears to be very stable upon repeated H_2S exposure at room temperature. This is a desirable property for highly H_2S stable MOFs; previous studies of a series of related MIL materials (MIL-47(V), MIL-53(Al, Cr),[14] MIL-125(Ti))[45] led to the hypothesis that H_2S stability is enhanced for MOFs that do not contain open metal sites, which cannot undergo M–SH_2 ligation. Additionally, CO_2 adsorption isotherms at 196 and 303 K were measured after each H_2S exposure, prior a TSR step (Fig. S10). These experiments confirmed the retention of both the surface area (592.4±7.6 m^2 g^{-1}, Fig. S12) and the CO_2 adsorption capacity of the Mg-CUK-1 (5.93±0.12 mmol g^{-1}, Figure 5B).

As shown previously, Mg-CUK-1 demonstrates 'soft crystalline' behaviour, being flexible in the solid-state;[46] the pores relaxing upon H_2O adsorption/desorption.[24] Thus, we decided to investigate such a flexible behaviour when H_2S molecules are adsorbed in the pores of Mg-CUK-1. First, a fully dehydrated Mg-CUK-1 was saturated with H_2S (15 %vol. H_2S). Later, this sample was incompletely re-activated (by only flowing dry N_2 gas at 303 K for 10 minutes) to achieve a partially H_2S saturated sample. When PXRD experiments were performed, a shift in the position of the low-angle reflections (between 8–9° 2θ) was observed (see 6A). This suggested a flexible character of the structure upon H_2S adsorption/desorption, since the PXRD pattern (partially H_2S saturated) did not matched neither with the fully activated sample nor the water saturated sample (Figure 6).

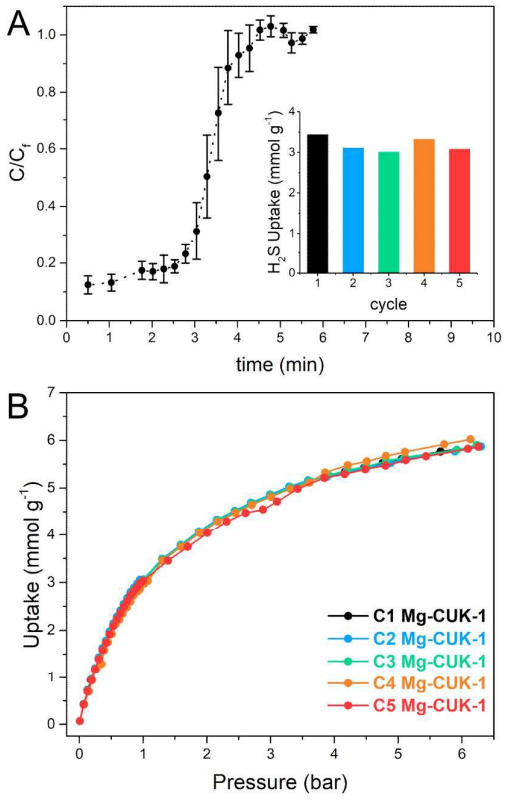

Figure 5. **(A)** Breakthrough curves for H_2S adsorption in Mg-CUK-1 at 303 K using a feed H_2S concentration of 15 %vol. The total H_2S/N_2 rate flow was 30 cm^3 min^{-1}. The inset shows the comparative adsorption capacities for each cycle. **(B)** The CO_2 adsorption isotherms for Mg-CUK-1 after H_2S sorption cycling, measured at 303 K and up to 6.5 bar.

View Article Online
DOI: 10.1039/C8TA05400B

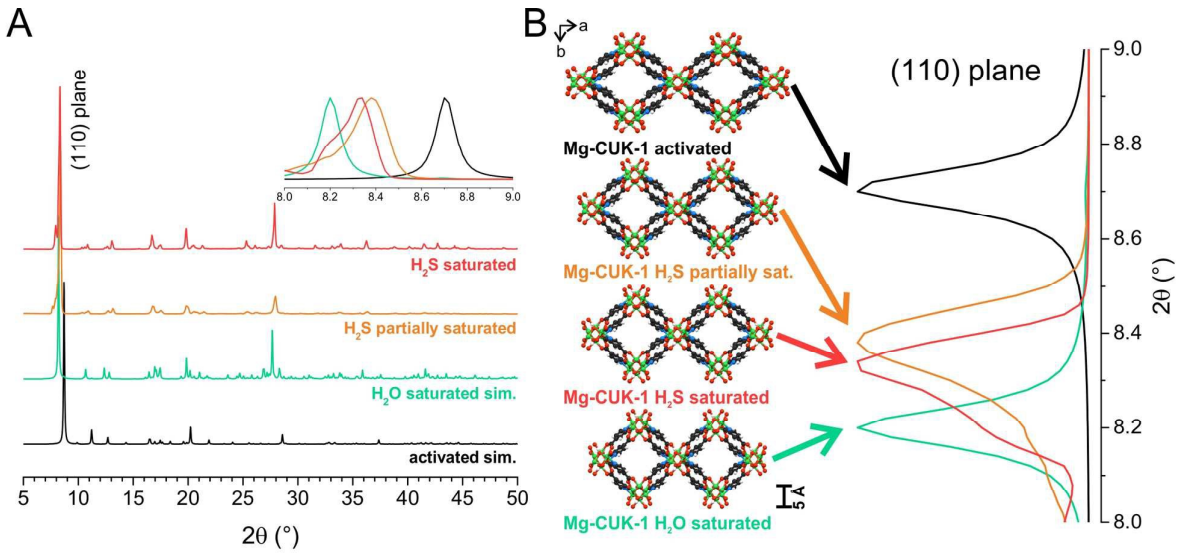

Figure 6. **(A)** PXRD experiments on samples of Mg-CUK-1 with different molecule loadings. The inset shows the two theta shifting of the 110 plane. (**B**) Representation of the Mg-CUK-1 cell deformation as a visual aid to explain the two theta shifting.

In order to gain a better understanding of the degree of the flexibility of Mg-CUK-1 upon H_2S loading, the experimental PXRD patterns collected at different H_2S loadings were analysed to extract the cell parameters of the H_2S-loaded material by the Le Bail methodology (FullProf program; see ESI).[47] From the cell parameters derived, plausible structural models for the partially and fully H_2S loaded phases were constructed starting with the crystal structure of the empty Mg-CUK-1 followed by a DFT-geometry optimization keeping fixed the experimental cell parameters. These calculations were performed using the same functional and basis set employed to initially geometry optimize the crystal structure of Mg-CUK-1.

Analysis of these plausible structural models indicated that the guest-induced evolution of the channel dimensions of Mg-CUK-1 (taking into consideration the van der Waals radius of the atoms, see ESI) is as follows: fully desolvated = 9.1 x 10.3 Å; H_2O saturated = 10.2 x 9.4 Å; partially H_2S loaded = 9.5 x 10.1 Å; H_2S saturated = 10.0 x 9.1 Å (Figure 6B). This trend is also consistent with an increase of the unit cell volume of the structure upon adsorption: fully desolvated = 2428.4 $Å^3$; partially H_2S loaded = 2518.0 $Å^3$; H_2O saturated = 2543.3 Å3; H_2S saturated = 2541.6 $Å^3$ corresponding to about 5% guest-induced unit cell volume change.

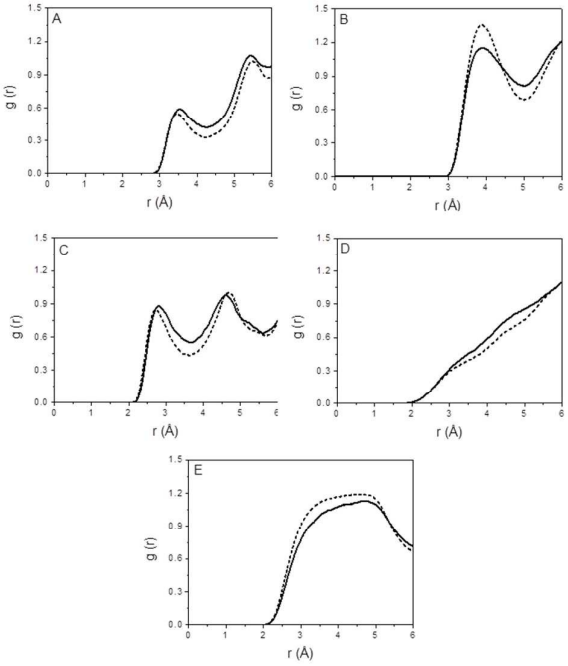

Figure 7. Radial distribution functions for the pairs $O_{\mu 3\text{-}OH}$ – S (**A**), O_{carb} – S (**B**), $H_{\mu 3\text{-}OH}$ – S (**C**), $O_{\mu 3\text{-}OH}$ – H_{H2S} (**D**), and S_{H2S} – H_{H2S} (**E**) in Mg-CUK-1 loaded with 1.08 (solid lines) and 4.89 (dashed lines) molecules of H_2S per unit cell at 303 K.

View Article Online
DOI: 10.1039/C8TA05400B

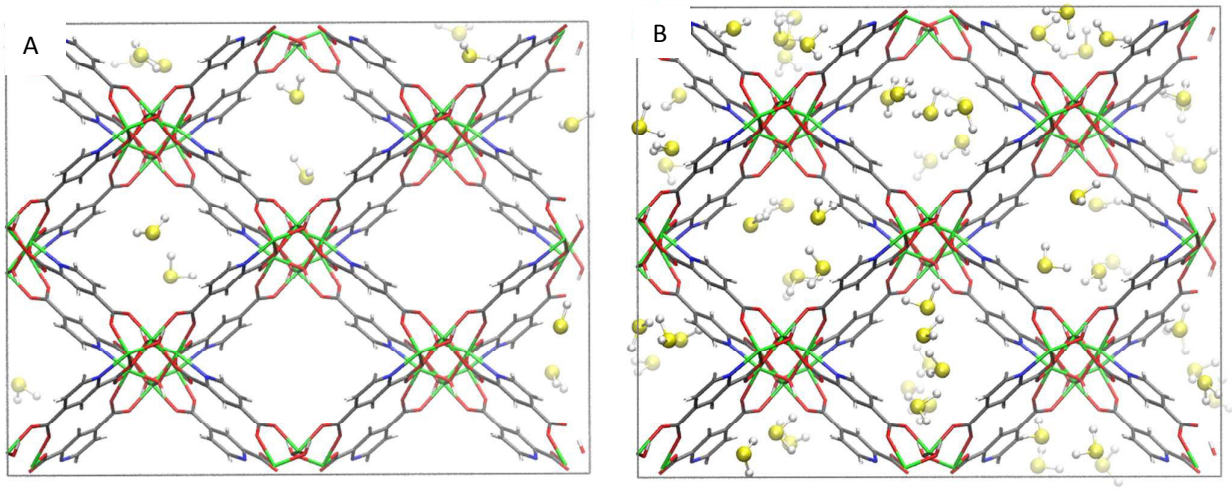

Figure 8. (A) Representative snapshots obtained from the GCMC simulations, showing the interactions between H_2S and the atoms of the MOF pore wall for 1.08 H_2S per unit cell; (**B**) the corresponding image for a higher loading of 4.89 H_2S per unit cell.

Finally, GCMC simulations were performed to gain in-depth insights into the adsorption of H_2S at the microscopic level. The calculated adsorption isotherm gave a maximum uptake of 5 mmol g^{-1}, which is somewhat higher than the experimentally observed value of 3.1 mmol g^{-1}. Our calculations further predicted an enthalpy of –23.3 kJ mol^{-1} for low-coverage adsorption, which is similar to the value reported for MIL-68(Al), another hydroxyl-based MOF material.[48] This moderately-strong interaction is primarily ascribed to interactions between H_2S molecules and the hydroxyl groups and O-atoms of the carboxylate groups, as confirmed by the plots of the radial distribution functions (RDFs; Figures 7A&B), which yield characteristic contact distances ranging from 3.3 Å to 4.0 Å. A corresponding snapshot showing the most preferential positions of H_2S molecules within the pores of Mg-CUK-1 at low coverage (1.08 H_2S *per* unit cell) is shown in Figure 8A. The RDF plots in Figures 7C&D show that the interactions between the hydroxyl groups and the H_2S molecules are established through relatively weak hydrogen bonds, in which the hydroxyls are the strongest hydrogen donor. This moderate H_2S···Mg-CUK-1 interaction is consistent with a relatively easy regeneration of the material after H_2S exposure and hence the reversible adsorption of this molecule. Upon increasing the theoretical H_2S loading from 1.08 to 4.89 molecules per unit cell, the calculated μ_3-OH···SH_2 distance only slightly shortened from 2.8 Å to 2.7 Å. Further, our calculations predicted that under higher H_2S loading, *inter*-molecular H_2S interactions tend to become slightly weaker (Figures 7E & 8B). This finding can be attributed to a certain degree of interaction of the H_2S molecules with the MOF pore-wall, which acts to prevent H_2S condensation inside the micropores, as shown in MIL-47(V).[14b]

Conclusions

The environmentally-friendly synthesised Mg-CUK-1 was demonstrated to be a highly robust MOF for acid gas remediation applications. Its chemically stability towards H_2O and H_2S (retention of the framework crystallinity and gas adsorption total capacity) was experimentally established by Powder X-ray diffraction and adsorption-desorption (H_2O and H_2S) experimental cycles. Mg-CUK-1 is one of the best performing H_2S breakthrough materials showing remarkable H_2S reversibility, under temperature swing re-activation (TSR) conditions. Remarkably the CO_2 adsorption properties of Mg-CUK-1 remain unchanged upon exposure to H_2O and H_2S. Mg-CUK-1 was shown to exhibit a 'soft crystalline' behaviour when small amounts of H_2S are confined within its micropores. Molecular simulations complemented our experimental evidence and more importantly, provided us the preferential sittings of CO_2 and H_2S molecules inside the channels of Mg-CUK-1. Particularly, the calculated moderate adsorption enthalpy for H_2S (–23.3 kJ mol^{-1}) in comparison to exiting MOF materials, confirmed the regeneration viability of Mg-CUK-1, under mild conditions. In summation, Mg-CUK-1 has been demonstrated to be an exceptional candidate for the capture of CO_2, even under humid conditions, as well as a remarkably stable adsorbent for the reversible sorption of H_2S.

Conflicts of interest

There are no conflicts of interest.

Acknowledgements

The authors thank Dr. A. Tejeda-Cruz (powder X-ray; IIM-UNAM) for analytical assistance, U. Winnberg (ITAM) for scientific discussions and G. Ibarra-Winnberg for conceptualising the design of this contribution. Financial support for this work was provided by PAPIIT UNAM Mexico (IN101517), CONACyT under grant Nos. 1789 (I.A.I.), 236879

View Article Online
DOI: 10.1039/C8TA05400B

(E.G.-Z.), 276862 (J.R.Á.) and 289042 (E.S.-G.), a scholarship from the National Counsel of Technological and Scientific Development CNPQ (P.G.M.M), the Institut Universitaire de France (G.M.), and the Welch Foundation (F-1738, J.E.R. & S.M.H.).

Notes and references

1 P. Kumar, K.-H. Kim, E. E. Kwon and J. E. Szulejko, *J. Mater. Chem. A*, 2016, **4**, 345.

2 (a) G. Maurin, C. Serre, A. Cooper and G. Férey, S. L. James, *Chem. Soc. Rev.*, 2017, **46**, 3104; (b) S. L. James, *Chem. Soc. Rev.*, 2003, **32**, 276; (c) J. L. C. Rowsell and O. M. Yaghi, *Microporous Mesoporous Mater.*, 2004, **73**, 3.

3 N. M. Padial, E. Quartapelle Procopio, C. Montoro, E. López, J. E. Oltra, V. Colombo, A. Maspero, N. Masciocchi, S. Galli, I. Senkovska, S. Kaskel, E. Barea and J. A. R. Navarro, *Angew. Chem. Int. Ed.*, 2013, **52**, 8290.

4 (a) K. Sumida, D. L. Rogow, J. A. Mason, T. M. McDonald, E. D. Bloch, Z. R. Herm, T. H. Bae and J. R. Long, *Chem. Rev.*, 2012, **112**, 724. (b) J. Liu, P. K. Thallapally, B. P. McGrail, D. R. Brown and J. Liu, *Chem. Soc. Rev.*, 2012, **41**, 2308. (c) D. Andirova, C. F. Cogswell, Y. Lei and S. Choi, *Microporous Mesoporous Mater.*, 2016, **219**, 276.

5 (a) E. Barea, C. Montoro and J. A. R. Navarro, *Chem. Soc. Rev.*, 2014, **43**, 5419; (b) M. S. Shah, M. Tsapatsis and J. I. Siepmann, *Chem. Rev.*, 2017, **117**, 9755.

6 (a) D. Britt, D. Tranchemontagne and O. M. Yaghi, *Proc. Natl. Acad. Sci. U. S. A.*, 2008, **105**, 11623; (b) C. A. Fernandez, P. K. Thallapally, R. K. Motkuri, S. K. Nune, J. C. Sumrak, J. Tian and J. Liu, *Cryst. Growth Des.*, 2010, **10**, 1037; (c) T. G. Glover, G. W. Peterson, B. J. Schindler, D. Britt and O. M. Yaghi, *Chem. Eng. Sci.*, 2011, **66**, 163; (d) S. Yang, J. Sun, A. J. Ramirez-Cuesta, S. K. Callear, W. I. F. David, D. P. Anderson, R. Newby, A. J. Blake, J. E.Parker, C. C. Tang and M. Schröder, *Nat. Chem.*, 2012, **4**, 887; (e) K. Tan, P. M. Canepa, W. Gong, J. Liu, D. H. Johnson, A. Dyevoich, P. K. Thallapally, T. Thonhauser, J. Li and Y. J. Chabal, *Chem. Mater.*, 2013, **25**, 4653; (f) W. P. III Mounfield, C. Han, S. H. Pang, U. Tumuluri, Y. Jiao, S. Bhattacharyya, M. R. Dutzer, S. Nair, Z. Wu, R. P. Lively, D. S. Sholl and K. S. Walton, *J. Phys. Chem. C*, 2016, **120**, 27230; (g) K. Tan, S. Zuluaga, H. Wang, P. M. Canepa, K. Soliman, J. Cure, J. Li, T. Thonhauser and Y. J. Chabal, *Chem. Mater.*, 2017, **29**, 4227; (h) S. Glomb, D. Woschko, G. Makhloufi and C. Janiak, *ACS Appl. Mater. Interfaces*, 2017, **9**, 37419.

7 (a) K. Vikrant, V. Kumar, K.-H. Kim and D. Kukkar, *J. Mater. Chem. A*, 2017, **5**, 22877; (b) J. F. Van Humbeck, T. M. McDonald, X. Jing, B. M. Wiers, G. Zhu and J. R. Long, *J. Am. Chem. Soc.*, 2014, **136**, 2432; (c) A. J. Rieth and M. Dincă, *J. Am. Chem. Soc.*, 2018, **140**, 3461.

8 (a) X. Zhang, W. Chen, W. Shi and P. Cheng, *J. Mater. Chem. A*, 2016, **4**, 16198; (b) A. C. McKinlay, B. Xiao, D. S. Wragg, P. S. Wheatley, I. L. Megson and R. E. Morris, *J. Am. Chem. Soc.*, 2008, **130**, 10440; (c) M. J. Ingleson, R. Heck, J. A. Gould and M. J. Rosseinsky, *Inorg. Chem.*, 2009, **48**, 9986. (d) A. C. McKinlay, J. F. Eubank, S. Wuttke, B. Xiao, P. S. Wheatley, P. Bazin, J.-C. Lavalley, M. Daturin, A. Vimont, G. De Weireld, P. Horcajada, C. Serre and R. E. Morris, *Chem. Mater.*, 2013, **25**, 1592; (e) S. R. Miller, E. Alvarez, L. Fradxourt, T. Devic, S. Wuttke, P. S. Wheatley, N. Steunou, C. Bonhomme, C. Gervais, D. Laurencin, R. E. Morris, A. Vimont, M. Daturi, P. Horcajada and C. Serre, *Chem. Commun.*, 2013, **49**, 7773; (f) R. R. Haikal, C. Hua, J. J. Perry, IV, D. O'Nolan, I. Syed, A. Kumar, A. H. Chester, M. J. Zaworotko, M. H. Yacoub and M. H. Alkordi, *ACS Appl. Mater. Interfaces*, 2017, **9**, 43520.

9 (a) L. Zhou, X. Zhang and Y. Chen, *Mater. Lett.*, 2017, **197**, 224; (b) K. Vellingiri, J. E. Szulejko, P. Kumar, E. E. Kwon, K.-H. Kim, A. Deep, D. W. Boukhvalov and R. J. C. Brown, *Sci. Rep.*, 2016, **6**, 27813.

10 (a) J.-R. Li, R. J. Kuppler and H.-C. Zhou, *Chem. Soc. Rev.*, 2009, **38**, 1477; (b) D. Banerjee, A. J. Cairns, J. Liu, R. K. Motkuri, S. K. Nune, C. A. Fernandez, R. Krishna, D. M. Strachan and P. K. Thallapally, *Acc. Chem. Res.*, 2015, **48**, 211; (c) K. Adil, Y. Belmabkhout, R. S. Pillai, A. Cadiau, P. M. Bhatt, A. H. Assen, G. Maurin and M. Eddaoudi, *Chem. Soc. Rev.*, 2017, **46**, 3402.

11 R. P. Pohanish, *Sittig's Handbook of Toxic and Hazardous Chemicals and Carcinogens*, William Andrew Publishing: New York, USA, 2008.

12 P. T. Anastas, J. C. Warner, *Green Chemistry: Theory and Practice*; Oxford University Press: Oxford, U.K., 1998.

13 (a) R. O. Beauchamp, J. S. Bus, J. A. Popp, C. J. Boreiko, D. A. Andjelkovich and P. Leber, *CRC Crit. Rev. Toxicol.*, 1984, **13**, 25. (b) P. K. Moore, M. Whiteman, *Chemistry, Biochemistry and Pharmacology of Hydrogen Sulfide*, Switzerland; P. K. Moore M. Whiteman, *Handbook of Experimental Pharmacology*, Springer International Publishing, 2015.

14 (a) L. Hamon, C. Serre, T. Devic, T. Loiseau, F. Millange, G. Férey and G. De Weireld, *J. Am. Chem. Soc.*, 2009, **131**, 8775; (b) L. Hamon, H. Leclerc, A. Ghoufi, L. Oliviero, A. Travert, J.-C. Lavalley, T. Devic, C. Serre, G. Férey, G. De Weireld, A. Vimont and G. Maurin, *J. Phys. Chem. C,* 2011, **115**, 2047.

15 J. Liu, Y. Wei, P. Li, Y. Zhao and R. Zou, *J. Phys. Chem. C*, 2017, **121**, 13249.

16 Y. Belmabkhout, R. S. Pillai, D. Alezi, O. Shekhah, P. M. Bhatt, Z. Chen, K. Adil, S. Vaesen, G. De Weireld, M. Pang, M. Suetin, A. J. Cairns, V. Solovyeva, A. Shkurenko, O. El Tall, G. Maurin and M. Eddaoudi, *J. Mater. Chem. A*, 2017, **5**, 3293.

17 R-T. Yang, in *Gas Separation by Adsoprtion Processes*, Imperial College Press: London, 1997, ch. 2, pp. 9-26.

18 (a) G. Liu, V. Chernikova, Y. Liu, K. Zhang, Y. Belmabkhout, O. Shekhah, C. Zhang, S. Yi, M. Eddaoudi and W. J. Koros, *Nat. Mater.*, 2018, **17**, 283; (b) M. Tagliabue, D. Farrusseng, S. Valencia, S. Aguado, U. Ravon, C. Rizzo, A. Corma and C. Mirodatos, *Chem. Eng. J.*, 2009, **155**, 553.

19 (a) E. González-Zamora and I. A. Ibarra, *Mater. Chem. Front.*, 2017, **1**, 1471; (b) T. Devic and C. Serre, *Chem. Soc. Rev.*, 2014, **43**, 6097; (c) A. J. Howarth, Y. Liu, P. Li, Z. Li, T. C. Wang, J. T. Hupp and O. K. Farha, *Nat. Rev. Mater.*, 2016, **1**, 15018; (d) C. R. Wade, T. Corrales-Sanchez, T. C. Narayan and M. Dincă, *Energy Environ. Sci.*, 2013, **6**, 2172; (e) S. M. T. Abtab, D. Alezi, P. M. Bhatt, A. Shkurenko, Y. Belmabkhout, H. Aggarwal, Ł. J. Weselinski, N. Alsadun, U. Samin, M. N. Hedhili and M. Eddaoudi, *Chem.*, 2018, **4**, 94; (f) M. W. Logan, J. D. Adamson, D. Le and F. J. Uribe-Romo, *ACS Appl. Mater. Interfaces*, 2017, **9**, 44529.

20 (a) F. Meunier, *Appl. Therm. Eng.*, 2013, **61**, 830. (b) C. Janiak and S. K. Henninger, *Chimia (Aarau).*, 2013, **67**, 419.

21 H. Furukawa, F. Gándara, Y.-B. Zhang, J. Jiang, W. L. Queen, M. R. Hudson and O. M. Yaghi, *J. Am. Chem. Soc.*, 2014, **136**, 4369.

22 (a) J. Liu, F. Zhang, X. Zou, G. Yu, N. Zhao, S. Fan and G. Zhu, *Chem. Commun.*, 2013, **49**, 7430. (b) M. Sánchez-Serratos, P. A. Bayliss, R. A. Peralta, E. González-Zamora, E. Lima and I. A. Ibarra, *New J. Chem.*, 2016, **40**, 68.

23 (a) M. Sadakiyo, T. Yamada and H. Kitagawa, *J. Am. Chem. Soc.*, 2014, **136**, 13166; (b) M. Sadakiyo, T. Yamada, K. Honda, H. Matsui and H. Kitagawa, *J. Am. Chem. Soc.*, 2014, **136**, 7701; (c) P. Ramaswamy, N. E. Wong and G. K. H. Shimizu, *Chem. Soc. Rev.*, 2014, **43**, 5913; (d) P. Ramaswamy, N. E. Wong, B. S. Gelfand and G. K. H. Shimiz, *J. Am. Chem. Soc.*, 2015, **137**, 7640; (e) S. S. Nagarkar, S. M. Unni, A. Sharma, S. Kurungot and S. K. Ghosh, *Angew. Chem.*, 2014,

DOI: 10.1039/C8TA05400B

126, 2676; D. D. Borges, S. Devautour-Vinot, H. Jobic, J. Ollivier, F. Nouar, R. Semino, T. Devic, C. Serre, F. Paesani and G. Maurin, *Angew. Chem. Int. Ed.*, 2016, **55**, 3919; (g) P. G. M. Mileo, S. Devautour-Vinot, G. Mouchaham, F. Faucher, A. Vimont, and G. Maurin, *J. Phys. Chem. C*, 2016, **120**, 28374.

24 B. Saccoccia, N. W. Waggoner, K. Cho, S. Lee, D. Hong, M. Alisha, V. M. Lynch, J. Chang and S. M. Humphrey, *Angew. Chem. Int. Ed.* 2015, **54**, 5394.

25 J. Woong, S. H. Jhung, Y. K. Hwang, S. M. Humphrey, P. T. Wood and J.-S. Chang, *Adv. Mater.*, 2007, **19**, 1830.

26 J. P. Perdew, K. Burke and M. Ernzerhof, *Phys. Rev. Lett.*, 1996, **77**, 3865.

27 (a) W. J. Hehre, J. A. Ditchfield and J. A. Pople, *J. Chem. Phys.*, 1972, **56**, 2257; (b) C. Campañá, B. Mussard and T. K. Woo, J. *Chem. Theory Comput.*, 2009, **5**, 2866.

28 J. G. Harris and K. H. Yung, *J. Phys. Chem.*, 1995, **99**, 12021.

29 J. L. F. Abascal and C. Vega, *J. Chem. Phys.*, 2005, **123**, 234505.

30 G. Kamath, N. Lubna and J. J. Potoff, *J. Chem. Phys.*, 2005, **123**, 124505.

31 A. K. Rappe, C. J. Casewit, K. S. Colwell, W. A. Goddard and W. M. Skiff, *J. Am. Chem. Soc.*, 1992, **114**, 10024.

32 S. L. Mayo, B. D. Olafson and W. A. Goddard, *J. Phys. Chem.*, 1990, **94**, 8897.

33 (a) E. Sánchez-González, P. G. M. Mileo, J. R. Álvarez, E. González-Zamora, G. Maurin and I. A. Ibarra, *Dalton Trans.*, 2017, **46**, 15208; (b) D. D. Borges, P. Normand, A. Permiakova, R. Babarao, N. Heymans, D. S. Galvão, C. Serre, G. De Weireld and G. Maurin, *J. Phys. Chem. C*, 2017, **121**, 26822;

34 (a) O. N. Osychenko, G. E. Astrakharchik and J. Boronat, *Mol. Phys.*, 2012, **110**, 227; (b) J. Kolafa and J. W. Perram, *Mol. Sim.*, 1992, **9**, 351.

35 T. J. H. Vlugt, E. García-Perez, D. Dubbeldam, S. Ban and S. Calero, *J. Chem. Theory Comput.*, 2008, **4**, 1107.

36 (a) H. Kim, S. R. Rao, E. A. Kapustin, L. Zhao, S. Yang, O. M. Yaghi and E. N. Wang, *Nat. Commun.*, 2018, **9**, 1191; (b) H. Kim, S. Yang, S. R. Rao, S. Narayanan, E. A. Kapustin, H. Furukawa, A. S. Umans, O. M. Yaghi and E. N. Wang, *Science*, 2017, **356**, 430.

37 A. Cadiau, J. S. Lee, D. D. Borges, P. Fabry, T. Devic, M. T. Wharmby, C. Martineau, D. Foucher, F. Taulelle, C.-H. Jun, Y. K. Hwang, N. Stock, M. F. De Lange, F. Kapteijn, J. Gascon, G. Maurin, J.-S. Chang and C. Serre, *Adv. Mater.*, 2015, **27**, 4775.

38 A. J. Rieth, S. Yang, E. N. Wang and M. Dincă, *ACS Cent. Sci.*, 2017, **3**, 668.

39 (a) J. R. Álvarez, R. A. Peralta, J. Balmaseda, E. González-Zamora and I. A. Ibarra, *Inorg. Chem. Front.*, 2015, **2**, 1080; (b) E. Sánchez-González, J. R. Álvarez, R. A. Peralta, A. Campos-Reales-Pineda, A. Tejeda-Cruz, E. Lima, J. Balmaseda, E. González-Zamora and I. A. Ibarra, *ACS Omega*, 2016, **1**, 305; (c) R. A. Peralta, B. Alcántar-Vázquez, M. Sánchez-Serratos, E. González-Zamora and I. A. Ibarra, *Inorg. Chem. Front.*, 2015, **2**, 898.

40 (a) X. Zhao, B. Xiao, A. J. Fletcher, K. M. Thomas, D. Bradshaw and M. J. Rosseinsky, *Science*, 2004, **306**, 1012; (b) H. J. Choi, M. Dincă and J. R. Long, *J. Am. Chem. Soc.*, 2008, **130**, 7848.

41 R. Roque-Malherbe, *Microporous Mesoporous Mater.*, 2000, **41**, 227.

42 R. A. Peralta, A. Campos-Reales-Pineda, H. Pfeiffer, J. R. Álvarez, J. A. Zárate, J. Balmaseda, E. González-Zamora, A. Martínez, D. Martínez-Otero, V. Jancik and I. A. Ibarra, *Chem. Commun.*, 2016, **52**, 10273.

43 (a) D.-M. Chen, X.-P. Zhang, W. Shi and P. Cheng, *Inorg. Chem.*, 2015, **54**, 5512; (b) G. E. Cmarik, M. Kim, S. M. Cohen and K. S. Walton, *Langmuir*, 2012, **28**, 15606; (c) D.-M. Chen, N.-N. Zhang, C.-S. Liu, Z.-H. Jiang, X.-D. Wang and M. Du, *Inorg. Chem.*, 2017, **56**, 2379.

44 (a) A. C. Kizzie, A. G. Wong-Foy and A. J. Matzger, *Langmuir* 2011, **27**, 6368; (b) J. A. Mason, T. M. McDonald, T.-H. Bae, J. E. Bachman, K. Sumida, J. J. Dutton, S. S. Kaye and J. R. Long, *J. Am. Chem. Soc.*, 2015, **137**, 4787; (c) V. Benoit, N. Chanut, R. S. Pillai, M. Benzaqui, I. Beurroies, S. Devautour-Vinot, C. Serre, N. Steunou, G. Maurin and P. L. Llewellyn, *J. Mater. Chem. A*, 2018, **6**, 2081.

45 S. Vaesen, V. Guillerm, Q. Yang, A. D. Wiersum, B. Marszalek, B. Gil, A. Vimont, M. Daturi, T. Devic, P. L. Llewellyn, C. Serre, G. Maurin and G. De Weireld, *Chem. Commun.*, 2013, **49**, 10082.

46 Y. Hijikata, S. Horike, D. Tanaka, J. Groll, M. Mizuno, J. Kim, M. Takata and S. Kitagawa, *Chem. Commun.*, 2011, **47**, 7632.

47 (a) Y. Laligant, A. Le Bail and F. Goutenoire, *J. Solid State Chem.*, 2001, **159**, 223; (b) T. Riosnel, J. Gonzalez-Platas and J. Rodriguez-Carvajal, WinPlotr and FullProf suite program, version 3.00. 2015; https://www.ill.eu/sites/fullprof (june, 2017).

48 Q. Yang, S. Vaesen, M. Vishnuvarthan, F. Ragon, C. Serre, A. Vimont, M. Daturi, G. De Weireld and G. Maurin, *J. Mater. Chem.*, 2012, **22**, 10210.